The Impact of the New Nuclear Data Libraries on the Isothermal Reactivity Coefficient Determination

Adimir dos Santos and Graciete Simões de Andrade e Silva

Instituto de Pesquisas Energéticas e Nucleares
Av. Prof. Lineu Prestes, 2242 CEP 05508-000
São Paulo, SP, Brazil
asantos@ipen.br

Abstract – *The impact of the new released evaluations for ^{235}U, ^{238}U, ^{16}O, and S(α,β) for hydrogen bound water, in the determination of the isothermal reactivity coefficient of thermal reactors fueled with slightly enriched uranium is addressed in this work. The experiment to serve as a benchmark for this kind of reactor response is the inversion point of the isothermal reactivity coefficient of the IPEN/MB-01 reactor which was recently approved to be included in the IRPhE handbook. The theoretical analyses have been performed employing the coupled NJOY/AMPX-II/TORT systems. The analyses reveal that the major impacts are due to new data of ^{235}U and to those of S(α,β) for hydrogen bound in water. The (C-E)/E values when considering the new data from these libraries show an excellent progress in the theoretical determination of this very important reactor response. The new data for ^{238}U and ^{16}O show very little impact on the analysis. This work supports the developments recently adopted in the generation of the new nuclear data libraries for ^{235}U and for the S(α,β) for hydrogen bound in water.*

I. INTRODUCTION

New evaluations for ^{235}U[1], ^{238}U[2,3], ^{16}O[4], and S(α,β) for hydrogen bound[5] in water were recently completed and made available for the reactor physics community. These new nuclear data are now under several benchmark tests and verifications and they will become important part of the future nuclear data libraries for which new releases are expected to be in 2017.

The nuclear data of great importance to this work are the ones of ^{235}U and those of hydrogen bound in water (S(α,β)). Particularly to the case of ^{235}U, the main objective of this new evaluation was to address issues with capture cross section and standard fission cross section values. This new evaluation incorporates new cross-section measurements done at LANL[6], RPI[7] and at the n_TOF located at the European Organization for Nuclear Research (CERN) in Geneva[8]. The thermal cross sections are of great importance to this work. A comparison of the thermal values, energy at 0.0253 eV, between the new ^{235}U evaluation and the ENDF/B-VII.1 is shown in Table I. The ENDF/B-VII.1 thermal capture is lower than that of the new evaluation by about 0.64 %, the scattering is higher by about 7.27 %, whereas the fission is essentially the same on both evaluations. The capture-to-fission ratio for ENDF and the new evaluation are 0.1687 and 0.1698, respectively. These changes together with the new evaluation of the S(α,β) for hydrogen bound in water performed in Bariloche, Argentina are the main causes that lead to the improvements on the temperature effects in thermal reactor calculations fueled with low enriched uranium.

Table I: Standard Values and Resonance Parameters Results

Cross Section	New Evaluation (barns)	ENDF/B-VII.1 (barns)
Fission	584.417	584.897
Capture	99.231	98.664
Scattering	14.086	15.112

Regarding the S(α,β) for hydrogen bound in water performed in Bariloche, the main differences from ENDF/B-VII.0 are the introduction of a molecular diffusion model for the translational motion and a continuous frequency spectrum computed from molecular dynamics simulations, which was computed for each temperature. The thermal scattering law was evaluated down to 10 °C. The ENDF/B-VII.0 considers these data only at 20 °C.

The choice of appropriate benchmarks to verify the adequacy of these evaluations in the determination of specific reactor response is crucial for the establishment of their accuracy. The purpose of this paper is to address the impact of these new nuclear data evaluations in the determination of a very important reactor response related to the safety of the facility; i.e., the isothermal reactivity coefficient. The verification analyses performed in this work considered thermal reactor fueled with uranium slightly enriched.

The benchmark chosen to cope with this task is the inversion point of the isothermal reactivity coefficient of the IPEN/MB-01 reactor[9,10]. This benchmark was approved to be included in the IRPhE handbook March 2017 edition[11]. By definition, the inversion point of the isothermal reactivity coefficient is the temperature where this reactor response becomes positive. According to its definition, the inversion point is believed to have the same sort of

sensitivity to the thermal and sub thermal [235]U cross sections as the isothermal reactivity coefficient of the IPEN/MB-01 reactor does. Several studies[12,13] made with the IPEN/MB-01 reactor core configuration suggest very high sensitivities of the isothermal reactivity coefficient of this system to the shape as well as to the magnitude of the thermal [235]U cross sections and to the $S(\alpha,\beta)$ for hydrogen bound in water. This facility has a lot of features that favor the neutron thermal energy region and several calculated responses have been found to be very sensitive to the thermal nuclear data particularly to those of the [235]U data.

The inversion point is an experimental quantity that was measured with an excellent level of accuracy due mainly to the very precise characteristics of the relative indicator of the control bank of the IPEN/MB-01 reactor and the temperature measurement and homogenization systems as well. Besides that, its experimental determination does not require any sort of calculated correction factors or any quantity that comes either from the calculation methodologies or from another experiment. For example, the measurements of the isothermal reactivity coefficients need the experimental determination of the reactivity. The reactivity between two points of temperature is not measured directly; instead it is inferred employing an inverse kinetics method together with a set of delayed neutron parameters. These last parameters are obtained either by numerical approach or by experiments. However, the delayed neutron parameters are physical quantities of very difficult experimental or numerical determination which will impose very restrictive uncertainty on the isothermal reactivity coefficient.

The IPEN/MB-01 research reactor is a zero power critical facility specially designed for measurements of a wide variety of reactor physics parameters to be used as benchmark experimental data for checking the calculation methodologies and related nuclear data libraries commonly used in the field of reactor physics. This facility is located in the city of São Paulo, Brazil and reached its first criticality on November 9, 1988. Since then it has been utilized for basic reactor physics research and as an instruction laboratory system. This facility consists of a 28x26 rectangular array of UO_2 fuel rods 4.3486 wt. % enriched uranium as UO_2 and clad by stainless steel (SS-304) inside a light water tank. The maximum allowed power is 100 W. The control of the IPEN/MB-01 reactor is via two control banks diagonally placed. The control banks are composed of 12 Ag-In-Cd rods and the safety banks by 12 B_4C rods. The square pitch of the IPEN/MB-01 reactor was chosen to be close to the optimum fuel-to-moderator ratio (maximum k_∞). This feature favors the thermal neutron energy region and mainly the [235]U events. Additional information regarding the IPEN/MB-01 reactor and facility is available in benchmark report LEU-COMP-THERM-077[14] for the standard core.

II. THE EXPERIMENT AND ITS THEORETICAL ANALYSIS

The experiments were performed employing three distinct IPEN/MB-01 reactor core configurations as shown in Fig. 1. Configuration A considers the standard core or the central 4x4 positions filled with fuel rods. Configuration B considers the central 4x4 positions filled with SS-304 rods. Configuration C considers the central 4x4 positions filled with water. Complete descriptions of the experimental determination of the inversion point of the isothermal reactivity coefficient can be found in Ref. 9 for configuration A and in Ref. 10 for configurations B and C. Here, the description will consider just the main points.
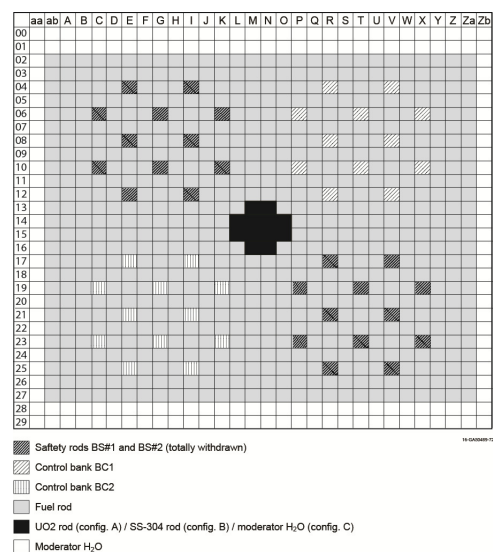
Fig. 1. Core configurations of the IPEN/MB-01 reactor.

The moderator tank was initially filled with cold water. The initial temperature and its range vary from configuration to configuration. For example for configuration A the initial temperature was nearly 8.5°C and it spans up to nearly 25.0 °C. For cases B and C, these data changed slightly. After filling the tank with cold water, the reactor system was allowed to reach thermal equilibrium. Fig. 2 shows schematically the control bank configuration for the experiment. The symbols X and Y in Fig. 2 represent, respectively, the BC1 and BC2 critical positions both in percent withdrawn. The control bank BC1 was kept fixed, respectively, at the 58.50%, 99.99 %, 67.00% withdrawn positions for configuration A, B, C.
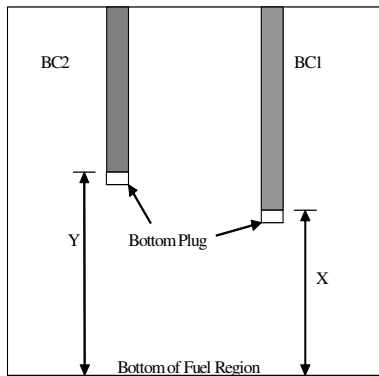
Fig. 2. Schematic axial representation of the control bank position.

The fine criticality control was achieved by the automatic control system continuously positioning the control bank BC2 around the true critical position. Fig. 3 shows the frequency of BC2 position against its position for a given critical state. This figure is similar to a Gaussian shape and shows that in the region labeled $\rho < 0$ (left side of the curve), the reactor system is subcritical, and conversely, in the region on the right hand side, $\rho > 0$, the reactor system is supercritical. The true critical position ($\rho = 0$) occurs at the maximum of this curve. This analysis was made for every critical configuration reported in this evaluation and the critical position at the maximum of each respective curve was considered to be the true BC2 control bank critical position. The *fluctuation spread* of the control bank position in this case has been taken equal to one standard deviation (1σ) of the Gaussian curve shown in Fig. 3. A typical value of the uncertainty of the relative control position indicator is 0.013 % of the withdrawn position, which represents 0.07 mm. In conclusion, the control bank position during the reactor operation can be acquired with a good level of accuracy.
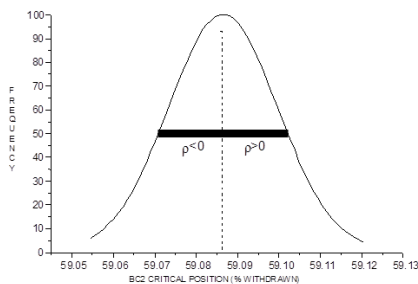
Fig. 3. Frequency of BC2 Control Rod Bank Position against its Position for a given Critical State and 1σ of Variations.

Most of the experiments were run at a power of 1W in order to have an appropriate detector signal-to-noise ratio. The experiment starts by heating the moderator water up to ~ 33°C by a heating/cooling system in a stepwise manner

between successive data acquisitions. The temperature spatial distribution in the reactor system was monitored by means of a set of thermocouples distributed in the core. For each step of the experiment, the system temperature was allowed to homogenize and stabilize, and after that the data (temperatures from all thermocouples and the control bank critical position) were recorded for further analysis. Extreme care was taken to guarantee the temperature homogenization in the reactor. The systematic and statistical uncertainties were taken into consideration in the analysis of the experimental data by an appropriate procedure.

The experimental data for configuration A is shown in Fig. 4. Configurations B and C show similar results. The horizontal and vertical bars showed in this figure represent 1σ of the statistical uncertainties on the BC1 control rod critical position and on the system temperature respectively. The statistical uncertainties are the spread of the measured data around the mean value. The systematic uncertainty is the calibration uncertainty being equal to 0.02 $^{\circ}$C for the temperature and 0.1 mm for the absolute control bank position.
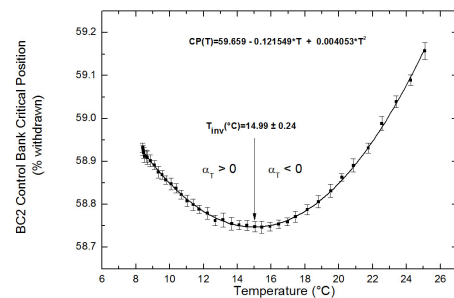
Fig. 4. BC2 Control bank critical position as a function of temperature for configuration A.

The experimental data shown in this figure were fitted in a 2nd order polynomial function by means of a least squares approach employing the CERN algorithm minuit2[15] together with the root data processing system (*https://root.cern.ch/*). This package can take into consideration the uncertainties on both the BC2 control bank critical position and on the temperature. The inversion point was found as the root of the derivative of the 2nd degree polynomial with respect to the temperature.

One can see on the Fig. 4 that a very small range of critical control bank positions achieved in the experiment. This makes difficult the experimental procedure for obtaining the inversion point. Moreover, a sensitivity analysis demonstrated that the control banks reactivity worth of the IPEN/MB-01 reactor (Ref.12) is not sensitive to the temperature variation, being very efficient neutron absorber. Therefore the whole reactivity variation relates to the fuel and reflector regions.

The final benchmark values for the inversion point of the isothermal reactivity coefficient (T_{inv})[11] for configurations A, B, and C are shown in Table II.

Table II. T_{inv} Benchmark Values

Configuration	Benchmark Value (°C)
A	14.99 ± 0.24
B	21.54 ± 0.24
C	22.36 ± 0.26

The proposed calculation approach described here was based on the author's experience that proposed and executed all the experimental work. The approach is to make k_{eff} calculations for a temperature range that covers the interval from the lowest to the highest temperature of the experimental data but in all these calculations keeping the control banks at their critical positions of 20 °C. All physical quantities that have temperature dependence such as cross sections (Doppler effect, $S(\alpha,\beta)$), material density (water for example), etc. must be taken into account in the analysis. Subsequently, the reactivity inserted by the temperature variation is calculated relative to the 20 °C case as:

$$\rho_i = \frac{(k_i - k_{20})}{(k_i \cdot k_{20})}, \qquad (1)$$

where k_i is the k_{eff} for temperature T_i and k_{20} is the k_{eff} at 20 °C. The theoretical determination of the inversion point is based on the behavior of this inserted reactivity as a function of temperature. The curve of reactivity versus temperature shows a maximum value whose temperature is the inversion point of the isothermal reactivity coefficient. The inversion point is found fitting this curve in a second order polynomial function and by imposing the derivative of the fitted second order polynomial equals to zero.

The theoretical analyses applied to the inversion point of the isothermal reactivity coefficient of the IPEN/MB-01 reactor were carried out in a deterministic approach employing the coupled NJOY/AMPX-II/TORT[16]. TORT k_{eff} calculations were considered for the entire temperature interval spanning from 2°C to 34°C in steps of 2°C for configuration A. The temperature interval for configurations B and C from 2°C to 34°C was kept the same but the temperature step was changed to 4°C from 34°C to 50°C.

The calculation methodology applied for the analyses of the inversion point of the isothermal reactivity coefficient of the IPEN/MB-01 reactor is shown in Fig. 5. This methodology has been applied successfully in Section 4.7 of IPEN(MB01)-LWR-RESR-001(LEU-COMP-THERM-077) in the analysis of the fission density distribution in the fuel rods of the IPEN/MB-01 reactor. The nuclear data libraries considered here are ENDF/B-VII.0 and the new evaluations for ^{235}U, ^{238}U, ^{16}O, and $S(\alpha,\beta)$ for hydrogen bound in water. Basically, starting from these nuclear data libraries, the

well-known NJOY system (version 99.90) was employed to access and to process the nuclear data file in a fine group structure. The thermal scattering law for hydrogen bound in water in the case of ENDF/B-VII.0 was obtained with LEAPR module of NJOY. The scattering laws for the new evaluation of the hydrogen bound in water were generated in CAB (Centro Atomico Bariloche, Argentina) and they were processed by the THERMR and GROUPR modules of NJOY. The nuclear data for all libraries were generated in the temperature interval needed for all configurations.
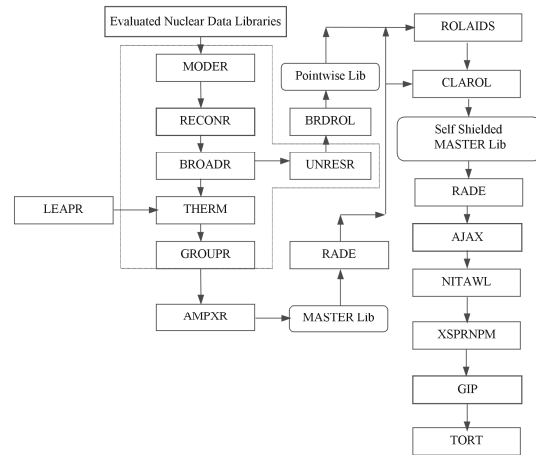
Fig. 5. Schematic Diagram for the Calculation Methodology.

The RECONR, BROADR, UNRESR, THERMR and GROUPR modules of NJOY are used in order to reconstruct and to Doppler broaden the cross sections, to calculate the self-shielding effects in the unresolved resonance region, to build the scattering matrices in the thermal region, and to transform these data into multigroup parameters, respectively. The next step was the production of a set of broad group energy library using the AMPX-II package. The pointwise and fine multigroup cross sections produced in the previous step are transferred to AMPX-II by two in house interface modules BRDROL and AMPXR. The mutual-shielding treatment of the actinide resolved resonances in the epthermal neutron energy region was carried out by ROLAIDS and the neutron spectra and subsequent cross section collapsing in the several regions of the IPEN/MB-01 reactor by XSDRNPM. ROLAIDS employs a collision probability method considering pointwise cross sections and takes into account both space and energy self shielding. The ROLAIDS method also considers the mutual shielding among the actinides present in the problem. XSDRNPM is a one-dimensional code and solves the transport equation using the S_N method. Firstly, the XSDRNPM cell model considered an infinite array of fuel pin square cells. The k_{inf} spectral calculations were performed in a cylindrical geometry in the fine group

structure considering a white boundary condition at the outer boundary of the cylindrized cell. The group cross sections for all nuclides were homogenized in a fine group level. Next, these data are merged with those of other regions such as radial, top and bottom reflectors and so on. Finally, XSDRNPM considers radial and axial slices of the IPEN/MB-01 reactor to get the final spectra for the broad group collapsing. The broad group cross sections of the control rods, guide tube, and bottom plugs were obtained using a super-cell model. This set of fine multigroup libraries was collapsed to a set of broad groups. At this point, the cross section library is problem dependent. The order of scattering (Legendre order expansion) was P_3 throughout the analysis. Finally, the broad group library is conveniently formatted to the TORT[17] (3D Discrete Ordinates Code) format using the GIP[18] program. Subsequently, with the broad group cross sections libraries previously generated; TORT performed k_{eff} calculations considering a fully three-dimensional geometric modeling of the IPEN/MB-01 reactor core.

The fully three-dimensional geometric setup for the TORT calculations was considered in the X-Y-Z geometry and P_3 approximation. The mesh distribution comprises 52 mesh intervals in X direction, 50 mesh intervals in Y direction, 81 mesh intervals in Z direction, for a total of 210,600 intervals. These intervals are represented by 10 numbers of material zones. The boundary conditions considered were void at top and bottom and at the left and right borders of the problem. The convergence criterion for the criticality calculations was set to the 1.00E-05 for the flux and the fission source and 1.00E-06 for the eigenvalue. As recommended in Ref.12, NJOY generated a library with 620 groups of energy. These data were collapsed in a srucutre of 16 groups by the module XSDRNPM of AMPX-II. TORT was run considering the 16 group structure with five thermal groups and for the S_N order 3. These were the group structure and S_N order to be used in the theoretical analyses of the inversion point of the isothermal reactivity coefficient of the IPEN/MB-01 reactor.

The whole pattern of calculations as shown in Fig. 5 (cross section generation and subsequent TORT k_{eff} calculations) was considered for the entire temperature interval spanning from 2°C to 50°C. The calculations were considered for every interval of 2°C up to 34°C and 4°C from 34°C to 50°C.; more precisely the cross section generation and TORT k_{eff} analysis were performed at 4°C, 6°C, 8°C and so forth up to the maximum temperature. Since the final result is the reactivity variation as a function of the temperature, the procedure adopted was based on keeping the control bank positions (BC1 and BC2) at the critical position of 20°C for all other temperatures and on the calculation of the reactivity variation relatively to the case of 20°C as the temperature changes. Finally, the NJOY/AMPX-II/TORT analyses follow all recommendations given in Ref. 12.

The TORT system was employed and a k-eigenvalue run was requested for a specific set of temperatures for each case considered in this evaluation. All the materials and regions specified in Section 3.5 of IPEN(MB01)-LWR-RESR-017[11] are modeled in the 3-D analyses. The reactivity relative to the case of 20°C was calculated employing Eq. (1).

III. RESULTS

Before proceeding to the discussions of the theory/experiment comparisons consider some illustrations of the results from the methodology NJOY/AMPX-II/TORT for the several temperatures considered in this evaluation. Table III shows k_{eff} and the reactivities relative to the 20°C case for configuration C employing the new data for ^{235}U, ^{238}U, ^{16}O and the S(α,β) for hydrogen bound in water. The remainder data were taken from ENDF/B-VII.0.

Table III. Calculated k_{eff} and Reactivities Relative to the 20°C Case for Configuration C.

Temperature (°C)	k_{eff}	Reactivity relative to 20°C Case (pcm)
2.0	1.000599	-64.68
4.0	1.000736	-51.00
6.0	1.000859	-38.72
8.0	1.000965	-28.14
10.0	1.001036	-21.05
12.0	1.001120	-12.67
14.0	1.001167	-7.98
16.0	1.001209	-3.79
18.0	1.001235	-1.20
20.0	1.001247	0.00
22.0	1.001226	-2.09
24.0	1.001234	-1.30
26.0	1.001220	-2.69
28.0	1.001199	-4.79
30.0	1.001173	-7.38
32.0	1.001093	-15.36
34.0	1.001050	-19.65
42.0	1.000852	-39.42
46.0	1.000669	-57.69
50.0	1.000447	-79.86

The reactivity as a function of the temperature was subsequently least-square fitted in a second order polynomial function as:

$$\rho(T) = A_0 + A_1 T + A_3 T^2 . \qquad (2)$$

The fitted polynomial coefficients and the corresponding covariance matrix for the polynomial coefficients are shown respectively in Tables IV and V.

$\rho(T)$ in Equation (2) represents the reactivity for a generic temperature T.

Table IV: The Polynomial Coefficients.

A_0	A_1	A_2
-72.86359	6.51559	-0.14554

Table V: The Covariance Matrix for the Polynomial Coefficients ($\sigma_{A_i A_j}$).

i\j	0	1	2
0	2.15317	-0.17321	0.00289
1	-0.17321	0.01784	-3.31466E-04
2	0.00289	-3.31466E-04	6.62725E-06

The inversion point can be determined as:

$$T_{inv} = -\frac{A_1}{2A_2}, \qquad (3)$$

and its error propagation to the inversion point is given by:

$$\sigma_{T_{inv}}^2 = \left(\frac{\partial T_{inv}}{\partial A_1}\right)^2 \sigma_{A_1}^2 + \left(\frac{\partial T_{inv}}{\partial A_2}\right)^2 \sigma_{A_2}^2 + 2\left(\frac{\partial T_{inv}}{\partial A_1}\right)\left(\frac{\partial T_{inv}}{\partial A_2}\right)\sigma_{A_1 A_2}, \quad (4)$$

where

$$\frac{\partial T_{inv}}{\partial A_1} = -\frac{1}{2A_2}, \qquad (5)$$

$$\frac{\partial T_{inv}}{\partial A_2} = \frac{A_1}{2A_2^2}, \qquad (6)$$

and σ_{A_1} , σ_{A2} , and $\sigma_{A_1 A_2}$ are the elements of the covariance matrix shown in Table V. The uncertainty in the theoretical inversion point arises from the least square approach. It is a property of the fitting data and the fitting function chosen to describe the phenomenon.

The theory/experiment comparisons for the inversion point of the isothermal reactivity coefficient of the IPEN/MB-01 reactor are shown in Tables VI through IX. The uncertainty in the calculated values arose from the least square approach. Fig. 6 illustrates in a graphical form the results of the calculated reactivities for configuration C. This figure shows the capability of the calculation approach adopted in this work to resolve the small reactivity range required to obtain the inversion point. The impact of the new libraries is explicitly shown as well.
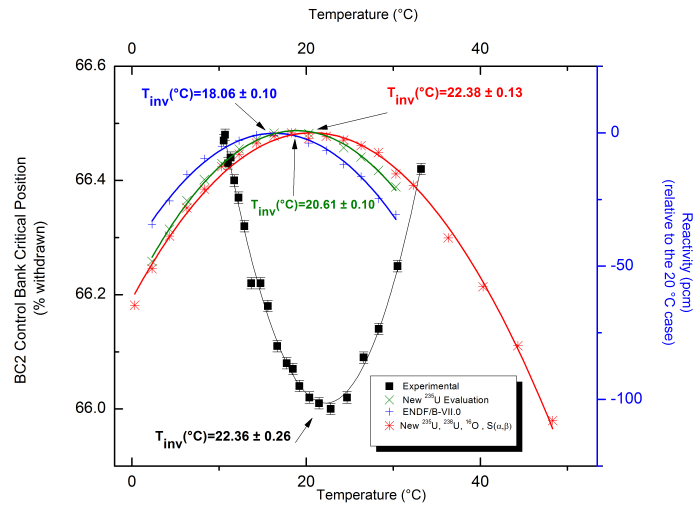
Fig. 6. Theory/Experiment Comparison of the Inversion Point of the Isothermal Reactivity Coefficient of the IPEN/MB-01 Reactor for Configuration C.

Table VI shows the analysis considering all nuclides from ENDF/B-VII.0. Table VII shows the results replacing the ^{235}U data to those of the new evaluation. Table VIII shows the results replacing the ^{235}U, ^{238}U, and ^{16}O data to those of new evaluations. Table IX shows the results replacing the ^{235}U, ^{238}U, ^{16}O data, and the S(α,β) for hydrogen bound in water to those of new evaluations. In all cases the remainder nuclides are from ENDF/B-VII.0 data. The error in the determination of the isothermal reactivity coefficient ($\alpha_{isoerror}$) was determined by noting that for every 1°C variation in the temperature scale there is a variation of nearly 0.416 ± 0.0031 pcm/°C[11] in the reactivity coefficient. Therefore, for example, for a variation of -4.30°C (ENDF/B/VII.0 case), there is a variation (or error) of -1.79 pcm/°C in the isothermal reactivity coefficient. This procedures was applied to all libraries and configurations considered in this work.

Table VI. Theory/Experiment Comparison Considering ENDF/B-VII.0

Configuration	Calculated T_{inv} (°C)	(C-E)/E±(1σ) (%)	$\alpha_{isoerror}$ (pcm/°C)
A	10.85 ± 0.20	-27.65 ± 1.80	1.72 ± 0.13
B	17.30 ± 0.10	-19.69 ± 1.00	1.76 ± 0.11
C	18.06 ± 0.10	-19.23 ± 1.05	1.79 ± 0.12

Table VII. Theory/Experiment Comparison Considering New Data for ^{235}U; remainders from ENDF/B-VII.0

Configuration	Calculated T_{inv} (°C)	(C-E)/E±(1σ) (%)	$\alpha_{isoerror}$ (pcm/°C)
A	13.25 ± 0.12	-11.63 ± 1.65	0.73 ± 0.11
B	19.81 ± 0.06	-8.04 ± 1.05	0.72 ± 0.10
C	20.61 ± 0.10	-7.86 ± 1.15	0.73 ± 0.12

Table VIII. Theory/Experiment Comparison Considering New Data for ^{235}U, ^{238}U and ^{16}O; remainders from ENDF/B-VII.0

Configuration	Calculated T_{inv} (°C)	(C-E)/E±(1σ) (%)	$\alpha_{isoerror}$ (pcm/°C)
A	13.20 ± 0.12	-11.96 ± 1.64	0.75 ± 0.11
B	19.80 ± 0.06	-8.09 ± 1.05	0.72 ± 0.10
C	20.66 ± 0.10	-7.62 ± 1.15	0.71 ± 0.12

Table IX. Theory/Experiment Comparison Considering New Data for ^{235}U, ^{238}U, ^{16}O, and S(α,β) for H in H_2O; remainders from ENDF/B-VII.0

Configuration	Calculated T_{inv} (°C)	(C-E)/E±(1σ) (%)	$\alpha_{isoerror}$ (pcm/°C)
A	14.25 ± 0.12	-4.97 ± 1.74	0.31 ± 0.11
B	21.74 ± 0.06	0.93 ± 1.15	-0.08 ± 0.10
C	22.38 ± 0.13	0.09 ± 1.28	-0.01 ± 0.12

Table VI shows that the (C-E)/E values are well outside of the 3σ range of their uncertainties. In spite of this very large deviation, the $\alpha_{isoerror}$ is a little bit over the desired accuracy (-1.0 pcm/°C)[19] for the determination of the reactivity determination. When the new data for ^{235}U replace those of ENDF/B-VII.0 (Table VII) the agreement between theory and experiment shows a good progress. The (C-E)/E values are still outside of the 3σ range of their uncertainties. However, the $\alpha_{isoerror}$ now attends the desired accuracy for the reactivity coefficient. Table VIII shows that the new data for ^{238}U and ^{16}O have very little impact on the determination of the isothermal reactivity coefficient. A very good progress in the determination of isothermal reactivity coefficient is found when the new nuclear data of ^{235}U, ^{238}U, ^{16}O, and S(α,β) for H in H_2O replace those of ENDF/B-VII.0 This comparison is shown in Table IX. Now, the (C-E)/E values are inside of the 3σ range of their uncertainties for all configurations. This is a very striking result never found before in other comparisons. The $\alpha_{isoerror}$ also attends the desired accuracy for the reactivity coefficient. The biggest T_{inv} deviation was found for configuration A. This configuration has the lowest inversion point and it is very sensitive to the nuclear data at lower temperatures. The S(α,β) evaluation from Bariloche was validated using data at room temperature, and it might have higher uncertainties as the temperature is reduced. This might explain the higher deviation found for configuration A.

IV. CONCLUSIONS

This work shows the usefulness of the benchmark of the inversion point of the isothermal reactivity coefficient of the IPEN/MB-01 reactor to test the adequacy of the nuclear data employed to determine the isothermal reactivity coefficient of thermal reactors fueled with slightly enriched uranium. The theoretical analyses as well as the nuclear data processing tasks have been successfully accomplished employing the coupled NJOY/AMPX-II/TORT systems. The analyses reveal that very good progress was obtained when the new evaluations for ^{235}U, and S(α,β) for hydrogen bound in water are considered in the determination of the inversion point of the isothermal reactivity coefficient of the IPEN/MB-01 reactor. The new data for ^{238}U and ^{16}O have very little impact in the isothermal reactivity determination. Particularly, Table IX shows that the $\alpha_{isoerror}$; i.e., the error in the determination of the isothermal reactivity coefficient satisfies with a great margin the desired accuracy (-1.0 pcm/°C) for this reactor response when the new data are considered in the analyses. As a general conclusion, this

work supports the changes promoted by these new nuclear data libraries in the determination of the isothermal reactivity coefficients of thermal reactors fueled with uranium slightly enriched.

REFERENCES

1. L. LEAL, G. NOGUERE, C. PARADELA, I. DURAN, L. TASSAN-GOT, Y. DANON, AND M. JANDEL, "Evaluation of the U235 Resonance Parameters to Fit the Standard Recommended Values," ND2016, September 11-16, 2016, Bruges, Belgium (2016).

2. P. SCHILLEBEEKX et al., "Evaluation of neutron induced reactions for U238 in the resonance region**,"** ND2016, September 11-16, 2016, Bruges, Belgium (2016).

3. H.I. KIM et al., "Neutron capture cross section measurements for ^{238}U in the resonance region at GELINA," *Eur. Phys. J.* A 52: 170 (2016).

4. L. LEAL, et al., "New R-Matrix Evaluation for ^{16}O from Thermal to 6 MeV," *Proc. PHYSOR 2016*, Sun Valley, Iadho, USA (2016) (CD-ROM).

5. J.I. MARQUEZ DAMIAN, J.R. GRANADA, D.C. MALASPINA, "CAB models for water: A new evaluation of the thermal neutron scattering laws for light and heavy water in ENDF-6 format," *Annals of Nuclear Energy*, **65**, 280 (2014).

6. Y. DANON, "Nuclear Data Measurements at RPI,"2011 Cross Section Evaluation Working Group Meeting, National Nuclear Data Center, Brookhaven National Laboratory, Upton, NY, November 16, 2011

7. T. A. JANDEL et al., "New Precision Measurements of the ^{235}U(n,γ) Cross Section," *Phys. Rev. Lett*. **109** (November 2012)

8. C. PARADELA et al. "High accuracy ^{235}U(n,f) data in the resonance region," The European Physical Journal, Vol. 111 (2016), WONDER-2015 4th International Workshop on Nuclear Data Evaluation for Reactor Application, Aix-en-Provence, France, 5-8 October 2015.

9. A. DOS SANTOS, H. PASQUALETO, L.C.C.B. FANARO, R. FUGA, AND R. JEREZ, "The Inversion Point of the Isothermal Reactivity Coefficient of the IPEN/MB-01 Reactor-1: Experimental Procedure," *Nucl. Sci. Eng.,* **133**, 314 (1999).

10. A. DOS SANTOS, et al., "New experimental results for the inversion point of the isothermal reactivity coefficient of the IPEN/MB-01 reactor," *Annals of Nuclear Energy,* **36**, 1740-1746, (2009).

11. A. DOS SANTOS, et al., IPEN(MB01)-LWR-RESR-017 "The Inversion Point of the Isothermal Reactivity Coefficient of the IPEN/MB-01 Reactor," NEA/NSC/DOC (95)03/I, Nuclear Energy Agency, Paris (March Edition) (2017).

12. A. DOS SANTOS, et al., "The Inversion Point of the Isothermal Reactivity Coefficient of the IPEN/MB-01

Reactor-2: Theoretical Analysis," *Nucl. Sci. Eng.,* **151**, 237 (2005).

13. A. DOS SANTOS, H. YORIYAZ, R. FUGA, R. JEREZ, "Reactivity Coefficients of IPEN/MB-01 Reactor," *Proc. PHYSOR 1996*, Mito, Ibaraki, Japan, September 16-20, 1996, **2,** E-141, Japan Atomic Energy Research Institute (CD-ROM).

14. A. DOS SANTOS, L.C.C.B. FANARO, M. YAMAGUCHI, R. JEREZ, G.S. ANDRADE E SILVA, P.T.D. SIQUEIRA, A.Y. ABE, R. FUGA, "LEU-COMP-THERM-077 Critical Loading Configurations of the IPEN/MB-01 Reactor," J. Blair Briggs, Ed., International Handbook of Evaluated Criticality Safety Benchmark Experiments, NEA/NSC/DOC (95)03/I, Nuclear Energy Agency, Paris (September Edition) (2004).

15 (http://seal.web.cern.ch/seal/snapshot/work-packages/mathlibs/minuit/).

16 A. DOS SANTOS, A.Y. ABE, A.G. MENDONÇA, L.C.C.B. FANARO, AND G.S. ANDRADE E SILVA, "Criticality Analysis Based on the Coupled NJOY/AMPX-II/TORT Systems," *Proc. Int. Conf. Physics of Nuclear Science and Technology*, Pittsburgh, Pennsylvania, May 7-12, 2000, American Nuclear Society (2000).

17. W. A. RHOADES, D. B. SIMPSON, "The TORT Three-Dimensional Discrete Ordinates Neutron/Photon Transport Code (TORT Version 3)," ORNL/TM-13221, (1991).

18. W. A. RHOADES, "The GIP Program for Preparation of Group-Organized Cross Section Libraries," Oak Ridge National Laboratory (1975).

19. J. BOUCHARD, C. GOLINELLI, H. TELLIER, "Besoins en Données Nucléaires pour les Réacteurs à Neutrons Thermiques, " *Proc. Int. Conf. Nuclear Data for Science and Technology*, Dordrecht (Netherlands), September 6-10, 1982, **1072**, 21, (1983).